Electronic Supplementary Material (ESI) for Energy & Environmental Science.

Electronic Supplementary Information

Photogeneration of Hydrogen from Water by a Robust Dye-Sensitized Photocathode

Table of Contents

EXPERIMENTAL SECTION

Sample Preparation

Materials. Zirconyl chloride octahydrate, 70% perchloric acid (99.999% purity), lithium perchlorate, tetrabutylammonium hexafluorophosphate (>99.0%), hydroxypropyl cellulose (Mw ~ 80,000, 20 mesh particle size), 2-(N-morpholino)ethanesulfonic acid (>99.5%; MES), sodium acetate and acetic acid (>99.7%) were used as received from Sigma-Aldrich. In_2O_3:Sn (ITO) dispersion in ethanol (TC8 DE, 20 wt%) was obtained from Evonik Industries. Ethanol (Decon Laboratories, 200 proof), methanol (anhydrous, 99%), acetonitrile (Optima LC/MS) and sodium hydroxide were purchased from Fisher Scientific. Distilled water was further purified with a Milli-Q ultrapure water purification system (Milli-Q water). Fluorine-doped tin oxide (FTO; resistance 15 Ω/cm^2) glass was purchased from Hartford Glass Inc. and cut into 10 mm x 40 mm strips as substrates for doctor-blading of metal oxide pastes. The chromophore ($[Ru^{II}(4,4'-(PO_3H_2)_2-2,2'-bipyridine)_2(2,2'-bipyridine)]Cl_2$; RuP_2^{2+}) and the electron donor (N,N,N',N'-$((CH_2)_3PO_3H_2)$4-4,4'-dianiline; DA) were synthesized according to the previously published procedures.[1,2] Loading solutions of RuP_2^{2+} (0.1 mM), DA (3.6 mM) and $ZrOCl_2$ (3 mM) were prepared by dissolving the compounds in 0.1 M perchloric acid (in Milli-Q water) and stored in the dark at room temperature before use. 5 mM NiP^{2+} was prepared by dissolving the NiP^{2+} in anhydrous methanol inside a N_2 purged glovebox. 0.1 M acetate buffer with pH 4.5 was prepared by mixing aqueous solutions of 0.1 M sodium acetate and 0.1 M acetic acid at 1:2 (v/v) ratio. 0.1 M MES buffer with pH 5.1 was prepared by titrating 0.1 M MES in water with 2 N NaOH to pH 5.1.

Synthesis of $[Ni(P^{Ph_2}N^{(C_6H_4CH_2PO_3H_2)_2})_2]^{2+}$. As shown in Scheme S1, complexes A[3] and B[4] were synthesized through a modified method from the published procedures with improved purity of the NiP^{2+} complex by the following additional procedures. A 50 mL Schlenk flask was charged with solid $[Ni(P^{Ph_2}N^{(C_6H_4CH_2PO_3H_2)_2})_2](Br)_2\bullet HBr$ (101.2 mg, 0.062 mmol) and 20 mL of degassed methanol. The solution was stirred for 10-15 min to completely dissolve the solid. Dry NEt_3 (1 equiv., 9 µL, 0.062 mmol) and AgOTf (2 equiv., 15.9 mg, 0.124 mmol) were added into the solution, and the reaction mixture was stirred for 12 h at room temperature. The volume of the solution was reduced to 10 mL. The solution was then filtered over dry Celite and dried under vacuum to afford the solid product. The solid was washed with dry CH_3CN (3 × 5 mL) and dried for 4 h to afford the final product (0.026 mmol., 43 mg, isolated yield 42%). $^{31}P\{^1H\}$ NMR (CD_3OD): δ 6.2 (s), 25.1 (s). ^1H NMR (CD_3OD): δ 7.46 (t, J = 8 Hz, 4H, Ph), 7.36 – 7.29 (m, 16H, Ph), 7.26 – 7.18 (m, 16H, Ph), 4.47 (d, J = 11 Hz, 8H, PCH_2N), 4.06 (d, J = 12 Hz, 8H, PCH_2N), 3.10 (d, J = 21 Hz, 8H, $C_6H_4CH_2P$). Elemental analysis: Calcd. for $C_{62}H_{70}N_4O_{18}F_6S_2NiP_8$: C,45.30; H, 4.29; N. 3.41. Found: C, 45.92; H, 4.11; N, 3.24. Cyclic voltammetry of $[Ni(P^{Ph_2}N^{(C_6H_4CH_2PO_3H_2)_2})_2](OTf)_2$ in MeOH (0.1 M $[Bu_4N]PF_6$) exhibits a reversible one-electron wave corresponding to the Ni(II/I) couple at $E_{1/2} = -0.75$ V vs. $Cp_2Fe^{+/0}$ and irreversible wave corresponding to the Ni(I/0) couple at $E_{pc} = -1.05$ V vs. $Cp_2Fe^{+/0}$.

Scheme S1

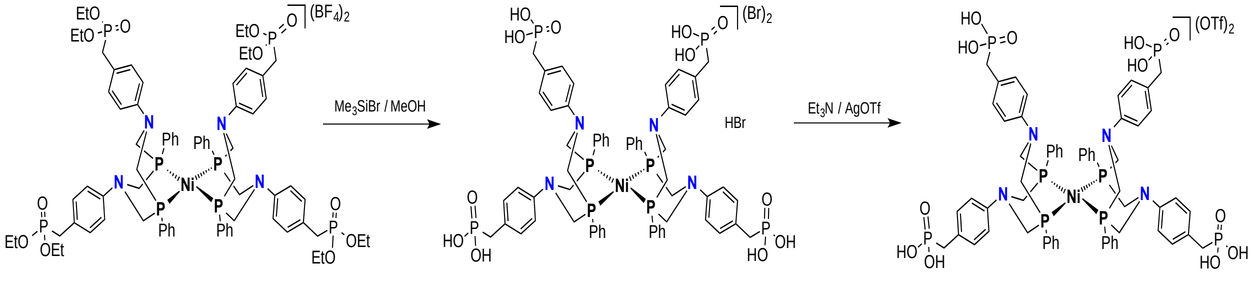

(A) (B) (C)

Mesoporous ITO and ZrO_2 Films. Mesoporous ZrO_2 and *nano*ITO thin films were prepared according to the published procedures with typical thickness of 3.5 μm.[5,6] The area of all films is 10 mm ×10 mm. Film thicknesses was measured using a Bruker Dektak XT profilometer.

Inverse Opal Macro-Mesoporous ITO (IO nanoITO) Films. The carboxyl-modified polystyrene latex spheres with 277 nm diameter were synthesized following a modification of the method of Fu et al.[7] The *IO nano*ITO films were made from modified published procedures.[8-10] Briefly, the ITO dispersion in ethanol (20 wt %) was mixed with 8.8 wt % suspension of hydroxypropyl cellulose in ethanol at 1:1 (v/v) ratio, followed by ultrasonication for 30 min. The synthesized carboxyl-modified polystyrene suspension was diluted to 8.0 wt % with water and mixed with the ITO-HPC colloid solution at 1:1 (v/v) ratio. The obtained suspension was ultrasonicated for 30 min, followed by stirring at room temperature for 3 days. The paste was then spread on FTO glass using the doctor-blade method with 3 layers of Scotch tape. The resulting films were dried at room temperature for 30 min and at 120°C in an oven for 30 min. The films were then heated to 450°C (at 2°C/min) and maintained at the temperature for 30 min to obtain the *IO nano*ITO films. Film thicknesses was approximately 6.5 μm measured by a Bruker Dektak XT profilometer.

Photocathode Assemblies. Sequential loading of layers was carried out by soaking the *nano*ITO or ZrO_2 films in DA (3.6 mM) for 12 hrs, $ZrOCl_2$ (3 mM) for 2 hrs, RuP_2^{2+} (0.1 M) for 12 hrs, $ZrOCl_2$ (3 mM) for 2 hrs, and NiP^{2+} (5 mM) for 12 hrs, in a stepwise manner. The loading times for *IO nano*ITO films were shorter with DA (3.6 mM) for 2 hrs, $ZrOCl_2$ (3 mM) for 2 hrs, RuP_2^{2+} (0.1 M) for 2 hrs, $ZrOCl_2$ (3 mM) for 2 hrs, and NiP^{2+} (5 mM) for 8 hrs. 0.1 M $HClO_4$ solution was used to rinse the films between switching to different loading solutions. NiP^{2+} was loaded onto dried films inside the N_2 purged glovebox. The photocathode assemblies prepared by this method have a structure of MO_X│-DA-Zr-RuP_2^{2+}-Zr-NiP^{2+} (FTO is omitted for simplicity). Control samples of MO_X│-DA-Zr-RuP_2^{2+} and MO_X│-RuP_2^{2+} were prepared by using the same conditions described above.

The tri-layered assembly structure on *IO nano*ITO surface was confirmed by examination of the surface coverages of RuP_2^{2+} and NiP^{2+} in the assemblies with and without loading of the Zr^{IV} bridges. There is only tiny amount of RuP_2^{2+} (< 5%) loaded on the *IO nano*ITO│-DA surface (without Zr bridge between DA and RuP_2^{2+}) and no NiP^{2+} loaded on *IO nano*ITO│-DA-Zr-RuP_2^{2+} (without Zr bridge between RuP_2^{2+} and NiP^{2+}). As comparison, the assembly built with Zr^{IV} bridges has a donor: dye: catalyst ratio of about 1.5: 1.5: 1 (Table S2), which proves the tri-layered structure on *IO nano* ITO surface. The integrities of RuP_2^{2+} and NiP^{2+} in the photocathode, *nano*ITO│-DA-Zr-RuP_2^{2+}-Zr-NiP^{2+}, were proven by UV-Vis absorption spectral analysis and spectroelectrochemistry of the photocathode, respectively, with comparison of those data for RuP_2^{2+} and NiP^{2+} in solutions.

Surface Loading Quantification

RuP_2^{2+}. Surface coverages (Γ in mol/cm^2) of RuP_2^{2+} were evaluated by UV-Vis absorption measurements on an Agilent 8453 UV-visible photodiode spectrophotometer with spectra recorded in pH 1 aqueous solutions. $\Gamma(RuP_2^{2+})$ was estimated according to $\Gamma = \Delta A_{465nm}/(\varepsilon_{465nm} \times 1000)$ with $\varepsilon_{465\ nm} = 16{,}800\ M^{-1}\ cm^{-1}$ determined from the solution spectrum of RuP_2^{2+} in pH 1 aqueous solution. UV-Vis absorption measurements for *nano*ITO and ZrO_2 samples were carried out directly on film samples, while the amount of RuP_2^{2+} on *IO nano*ITO samples was determined from the UV-Vis absorption spectra of dissolved RuP_2^{2+} in 2 N NaOH.

DA. In double-step chronocoulometry experiments, a potential step at 1.1 V vs NHE, past the two-electron oxidation of DA, was held until the oxidation was complete, followed by a reverse step at 0 V. Data were analyzed by using Anson plots of the charges passed versus $t^{1/2}$ for the forward and reverse steps.[11] Background charges were evaluated from the film samples without DA and were subtracted from the total charges of the DA samples. Surface coverages of DA were calculated from the charges of the two-electron oxidation of DA. Samples were purged with N_2 for at least 30 min prior to experimentation.

NiP^{2+}. Surface coverages of NiP^{2+} were determined by using a similar method as described above for Γ(DA). A forward potential step at -0.8 V vs NHE was applied to reduce the NiP^{2+} to NiP^0 in the double-step chronocoulometry experiments, followed by a reverse step at 0.0 V vs NHE. Anson plots of the charges passed versus $t^{1/2}$ for the forward and reverse steps were used for data analysis.[11] Background charges were subtracted from the samples without NiP^{2+}. Surface coverages of NiP^{2+} were calculated from the charges of the two-electron reduction of NiP^{2+}. All samples were purged with N_2 prior to experimentation.

Steady State Emission Measurement

Steady state emission spectra for MO_X|-RuP_2^{2+}, MO_X|-DA-Zr-RuP_2^{2+} and MO_X|-RuP_2^{2+}-Zr-NiP^{2+} samples were acquired with a PTI 4SE-NIR Quanta Master fluorimeter with 488 nm light excitation at room temperature. Samples were immersed in 0.1 M $LiClO_4$ acetonitrile solutions and degassed with N_2 for 30 min before measurements. Emitted light intensities were acquired and integrated from 520 nm to 800 nm with data shown in Fig. S5.

Nanosecond Transient Absorption (TA) Measurement

TA measurements were performed with a nanosecond transient absorption spectrometer which is based on a Nd:YAG (Spectra-Physics Quanta-Ray Lab-170) and OPO (VersaScan, 5−7 ns, 1 Hz, 0.5 cm beam diameter) laser system. The white light probe pulses were generated by a pulsed 450 W Xe lamp and passed through a 345 nm long pass filter before reaching the samples to avoid direct band gap excitation of the films. A 488 nm notch filter was placed before the detector to reject unwanted scattered excitation light. Single wavelength TA changes of the samples upon excitation by 488 nm laser pulses (3.7 mJ/pulse) were detected by a monochromator/PMT (Hamamatsu R928) system and monitored using a digital oscilloscope. Film samples with an area of 1.0 cm^2 were placed in a 1 cm pathlength quartz cuvette filled with MeCN/0.1 M $LiClO_4$ electrolyte. All samples were degassed with N_2 for 30 min before measurements. The data consisting of an 80-short average was analyzed by Origin Pro 2016 software.

Photocurrent and Dye-Sensitized Photoelectrocatalytic (DSPEC) H_2 Evolution Measurements

A custom made photoelectrochemical cell was used for photocurrent and DSPEC H_2 evolution measurements. The cell consists of two compartments (square Pyrex cuvette, inner diameter: 14 mm; wall thickness: 1.75 mm) separated by a nafion membrane, with one containing the dye-sensitized photocathode and the other having a platinum mesh counter electrode. A Ag/AgCl reference electrode was placed in the anodic compartment. The photocathode compartment was sealed by a Viton o-ring joint adaptor in between the threaded top of the glass compartment and a PEEK (polyether ether ketone) custom made threaded cap. In the middle of the cap, there were three drilled and taped ports, with one allowing electrical connection of the photocathode, one for a PEEK N_2 degassing tubing, and one for placing the needle tip of a H_2 microsensor (diameter 1.6 mm, Unisence, H_2-NP) for H_2 measurement in the headspace. All ports were gas-tight sealed with ferrules and threaded nuts (IDEX Health & Science). The hydrogen microsensor signal was amplified on a Unisense amplifier and was calibrated with 0%, 5% and 100% H_2 due to the linear response of the sensor in the range of 0 to 100% H_2. The calibration was performed before each DSPEC experiment and checked after the experiment to make sure no drift of the calibration curve. No change of the calibration data was observed within at least 24 hrs. The H_2 signal was also linearly converted to partial pressure for quantification of dissolved H_2 which was added to the amount of H_2 in the headspace for estimation of overall H_2 evolution. A CHI 601D electrochemical workstation was used to supply the -0.25 V vs NHE applied bias for the photocathode and also to record the current–time (i–t) signals. The photocathode active area (1 cm^2) was immersed in either pH 4.5, 0.1 M acetate buffer or pH 5.1, 0.1 M MES buffer, both of which were added with 0.4 M $NaClO_4$ supporting electrolyte to give an ionic strength of 0.5 M. The counter electrode compartment was filled with the same solution as that of the photocathode. Light illumination was provided by a solid-state light source (Lumencor, Inc.; λ_{max}: 445 nm, 20-nm FWHM, output: 5 mW; beam diameter: 0.8 cm) coupled to a Newport liquid light guide and focusing–imaging beam probe. The photocathode compartment was N_2 degassed through the PEEK tubing for 40 min, after which the degassing path was stopped from outside connection by a gas-tight Hamilton 3-way manual valve prior to DSPEC experiments. Constant stirring was kept during the PEC experiments.

Calculation of Quantum yield of H_2:

$$\eta_{QY} = \frac{n(H_2) * N_A * h * c * 2}{\lambda * t * I * A}$$

with n(H_2): moles of H_2 (moles), N_A: Avogadro constant (mol^{-1}), h: Planck constant (kg m^2 s^{-1}), c: speed of light (m s^{-1}), λ: wavelength (m), t: irradiation time (s), I: light intensity (W m^{-2}) and A: irradiated area (m^2). η_{QY} represents the efficiency of the photocathode in generating H_2 at the applied bias of -0.25 V vs NHE, based on the absorbed photons.

Calculation of Faradaic yield of H_2:

$$\text{Faradaic yield} = \frac{moles\ of\ H_2 \times 2}{moles\ of\ charges} \times 100\%,$$

with the moles of charges determined from the integration of the chronoamperometric curves with subtraction of the background charges.

Table S1 **Quenching efficiencies of $RuP_2^{2+}*$ by NiP^{2+} or DA in *nano*ITO samples.**

Assemblies	η_q
$-RuP_2^{2+}-Zr-NiP^{2+}$	89%
$-DA-Zr-RuP_2^{2+}$	95%

Table S2 **Surface coverages of molecules on *nano*ITO and *IO nano*ITO films.**

Assembly Films	Film Thickness / μm	Surface Coverage (Γ, nmol/cm^2)		
		DA	RuP_2^{2+}	NiP^{2+}
*nano*ITO│$-DA-Zr-RuP_2^{2+}-Zr-NiP^{2+}$	3.5	58 (±6.8)	58 (±6.6)	2.0 (±0.8)
*IO nano*ITO│$-DA-Zr-RuP_2^{2+}-Zr-NiP^{2+}$	6.3	89 (±7.3)	90 (±5.5)	61 (±7.1)

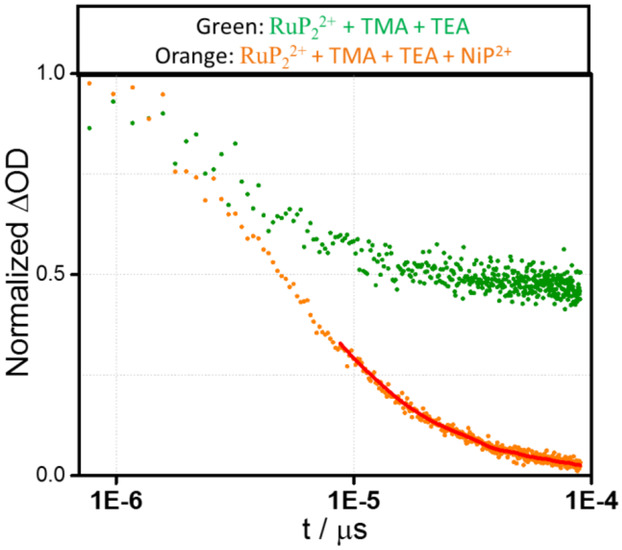

Fig. S1 Transient absorptive changes at 510 nm following excitation of RuP_2^{2+} + 0.04 M tri-p-tolylamine + 0.4 M triethylamine at 488 nm in N_2 degassed acetonitrile in the absence (green) and presence (orange) of NiP^{2+} (57 μM), showing the kinetics of reduction of NiP^{2+} by RuP_2^{+}. Scatter: TA data; red curve: fitted data using Origin Pro 2016 software according to second order kinetics. From the fitting, the second order rate constant of the reaction shown in eqn. S2 is 9×10^8 $M^{-1}s^{-1}$.

$$RuP_2^{2+} + TTA + TEA \xrightarrow{hv} RuP_2^{+} + TTA^{+\cdot} + TEA \rightarrow RuP_2^{+} + TTA + TEA^{+\cdot} \qquad \text{eqn. S1}^{12}$$

$$RuP_2^{+} + NiP^{2+} \rightarrow RuP_2^{2+} + NiP^{+} \qquad \text{eqn. S2}$$

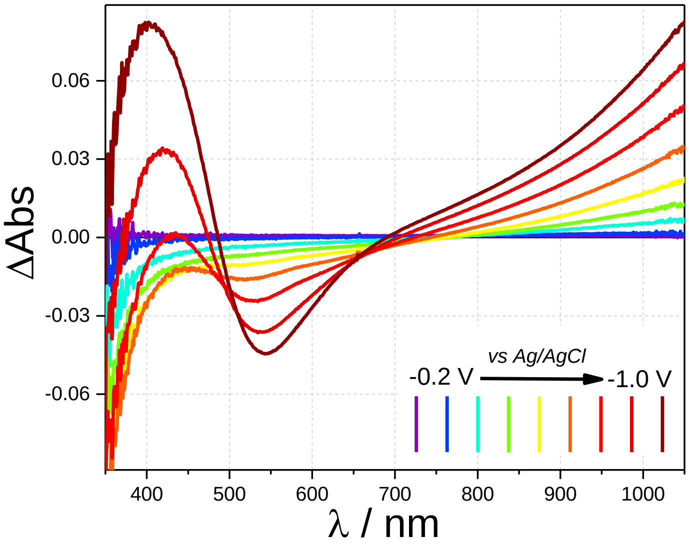

Fig. S2 Spectroelectrochemistry of NiP^{2+} on nanoITO under applied bias of -0.2 V— -1.0 V vs Ag/AgCl in N_2 degassed acetonitrile/0.1 M $TBA(PF_6)$. The absorption difference spectra include spectrophotometric changes of both reduced NiP^{2+} and reduced *nano*ITO under the negative bias.

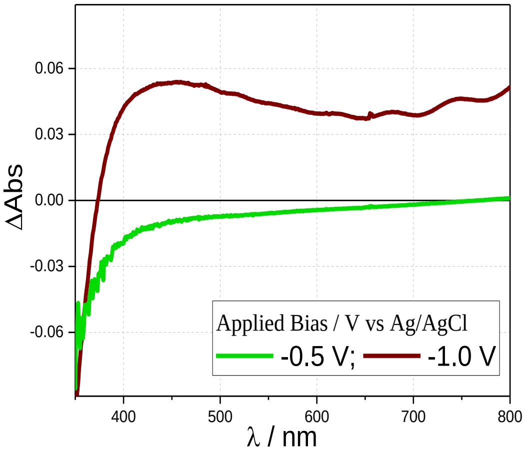

Fig. S3 Spectroelectrochemistry of *nano*ITO under -0.5 V and -1.0 V vs Ag/AgCl in N_2 degassed acetonitrile/0.1 M $TBA(PF_6)$.

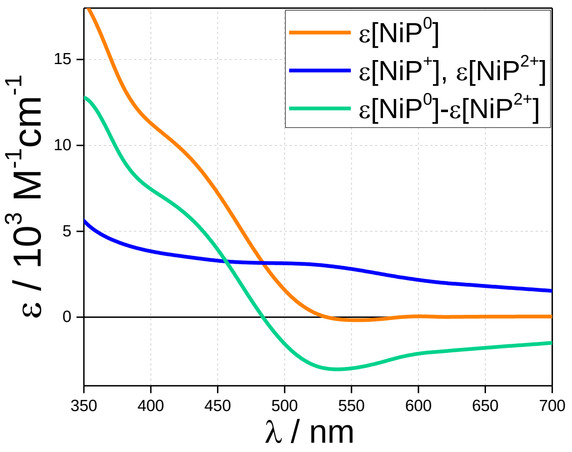

Fig. S4 Extinction coefficients of NiP^{2+}, NiP^{+} and NiP^{0} in acetonitrile. Data was obtained from spectroelectrochemistry and UV-Vis absorption spectra of NiP^{2+}.

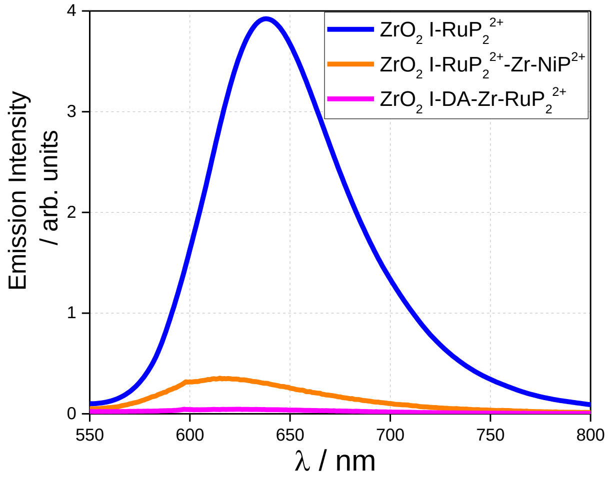

Fig. S5 Emission Spectra of $ZrO_2|$-RuP_2^{2+}, $ZrO_2|$-RuP_2^{2+}-Zr-NiP^{2+} and $ZrO_2|$-DA-Zr-RuP_2^{2+} samples in N_2 degassed acetonitrile /0.1 M $LiClO_4$ electrolyte under excitation at 488 nm.

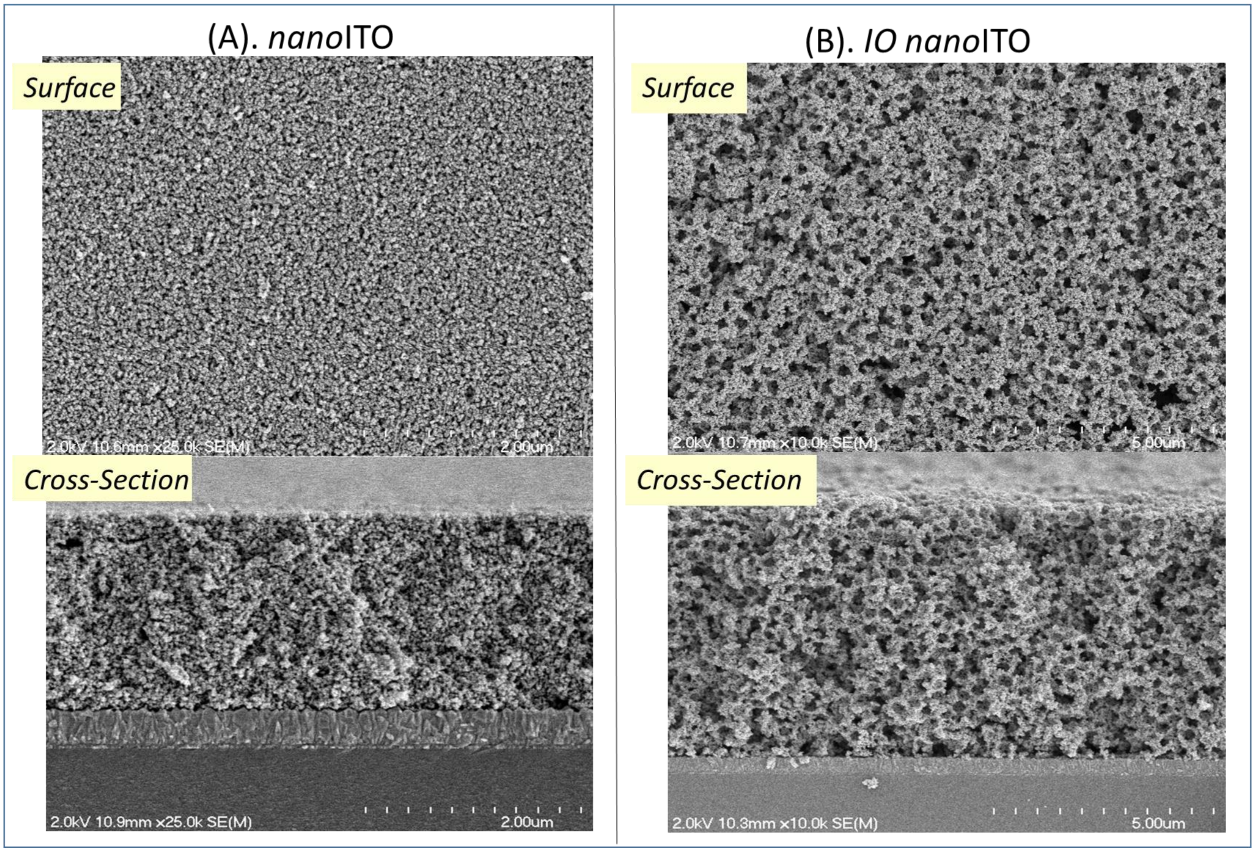

Fig. S6 SEM (scanning electron microscopy) images of (A) *nano*ITO and (B) *IO nano*ITO on FTO glass with scales of 2 μm and 5 μm, respectively. Top: surface; bottom: cross-section.

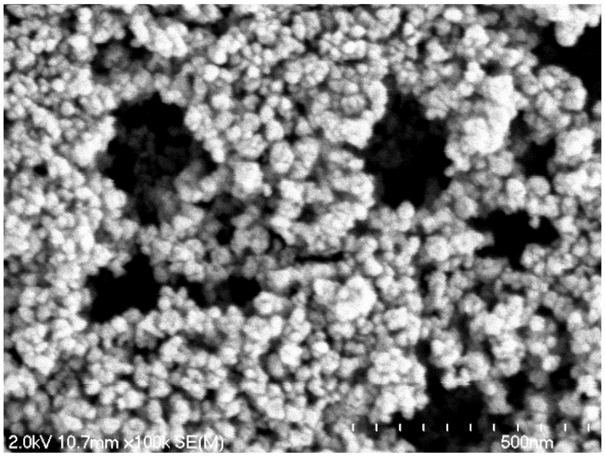

Fig. S7 Surface SEM image of *IO nano*ITO on FTO glass at 500 nm scale, showing an average macro-pore size of 225 nm.

References

1 M. R. Norris, J. J. Concepcion, C. R. K. Glasson, Z. Fang, A. M. Lapides, D. L. Ashford, J. L. Templeton and T. J. Meyer, *Inorg. Chem.*, 2013, **52**, 12492-12501 (DOI:10.1021/ic4014976).

2 B. H. Farnum, K. Wee and T. J. Meyer, *Nat. Chem.*, 2016, **8**, 845-852.

3 U. J. Kilgore, J. A. S. Roberts, D. H. Pool, A. M. Appel, M. P. Stewart, M. R. DuBois, W. G. Dougherty, W. S. Kassel, R. M. Bullock and D. L. DuBois, *J. Am. Chem. Soc.*, 2011, **133**, 5861-5872 (DOI:10.1021/ja109755f).

4 M. A. Gross, A. Reynal, J. R. Durrant and E. Reisner, *J. Am. Chem. Soc.*, 2014, **136**, 356-366 (DOI:10.1021/ja410592d).

5 T. A. Heimer, S. T. D'Arcangelis, F. Farzad, J. M. Stipkala and G. J. Meyer, *Inorg. Chem.*, 1996, **35**, 5319-5324 (DOI:10.1021/ic960419j).

6 B. H. Farnum, Z. A. Morseth, M. K. Brennaman, J. M. Papanikolas and T. J. Meyer, *J Phys Chem B*, 2015, **119**, 7698-7711 (DOI:10.1021/jp512624u).

7 S. Meng, D. Li, X. Fu and X. Fu, *J. Mater. Chem. A*, 2015, **3**, 23501-23511 (DOI:10.1039/C5TA06955F).

8 B. Hatton, L. Mishchenko, S. Davis, K. H. Sandhage and J. Aizenberg, *Proceedings of the National Academy of Sciences*, 2010, **107**, 10354-10359.

9 D. Mersch, C. Lee, J. Z. Zhang, K. Brinkert, J. Fontecilla-Camps, A. W. Rutherford and E. Reisner, *J. Am. Chem. Soc.*, 2015, **137**, 8541-8549 (DOI:10.1021/jacs.5b03737).

10 J. Du, X. Lai, N. Yang, J. Zhai, D. Kisailus, F. Su, D. Wang and L. Jiang, *ACS Nano*, 2011, **5**, 590-596 (DOI:10.1021/nn102767d).

11 A. Bard and L. Faulkner, *Electrochemical Methods: Fundamentals and Applications*, John Wiley & Sons, Inc, 2001.

12 B. Shan and R. Schmehl, *J Phys Chem A*, 2014, **118**, 10400-10406 (DOI:10.1021/jp503901v).